Chinese Journal of
POLYMER SCIENCE 高分子科学

Computer Simulation Study on Adsorption and Conformation of Polymer Chains Driven by External Force

Gao He-Bei, Li Hong, Zhang Xiao-Qin, Wang Xiang-Hong, Li Chao-Yang, Luo Meng-Bo

Cite this article as:
Gao He-Bei, Li Hong, Zhang Xiao-Qin, Wang Xiang-Hong, Li Chao-Yang, Luo Meng-Bo. Computer Simulation Study on Adsorption and Conformation of Polymer Chains Driven by External Force[J]. *Chinese J. Polym. Sci*, 2021, 39(2): 258-266. doi: 10.1007/s10118-020-2491-x

View online: https://doi.org/10.1007/s10118-020-2491-x

Chinese Journal of
POLYMER SCIENCE

ARTICLE

https://doi.org/10.1007/s10118-020-2491-x
Chinese J. Polym. Sci. **2021**, *39*, 258–266

Computer Simulation Study on Adsorption and Conformation of Polymer Chains Driven by External Force

He-Bei Gao[a], Hong Li[b*], Xiao-Qin Zhang[b*], Xiang-Hong Wang[a], Chao-Yang Li[c], and Meng-Bo Luo[d*]

[a] *Department of Information, Wenzhou Polytechnic, Wenzhou 325035, China*
[b] *College of Computer Science and Artificial Intelligence, Wenzhou University, Wenzhou 325035, China*
[c] *Department of Physics, Hangzhou Normal University, Hangzhou 310036, China*
[d] *Department of Physics, Zhejiang University, Hangzhou 310027, China*

Abstract In this work, Monte Carlo simulations are used to study the critical adsorption behaviors of flexible polymer chains under the action of an external driving force F parallel to an attractive flat surface. The critical adsorption temperature T_c decreases linearly with increasing F, indicating that the driving force suppresses the adsorption of polymer. The conformation of polymer is also affected by the driving force. However, the effect of F is dependent on the competition between the driving force and temperature. Under strong force or at low temperature, the polymer is stretched along the direction of the force, while under weak force or at high temperature, the polymer is not stretched. When the force is comparable to the temperature, the polymer may be stretched perpendicular to the driving force, and below T_c, we observe conformational transitions from parallel to perpendicular and again to parallel by decreasing the temperature. We found that the perpendicular stretched conformation leads the polymer chain to synchronously move along the direction of the driving force. Moreover, the conformational transitions are attributed to the competition and cooperation between the driving force and the temperature.

Keywords Critical adsorption; Polymer; Driving force; Conformation; Monte Carlo simulation

Citation: Gao, H. B.; Li, H.; Zhang, X. Q.; Wang, X. H.; Li, C. Y.; Luo, M. B. Computer simulation study on adsorption and conformation of polymer chains driven by external force. *Chinese J. Polym. Sci.* **2021**, *39*, 258–266.

INTRODUCTION

The adsorption of polymer chains has important applications in colloidal stability, surface coating, biocompatibility, wetting, liquid chromatography, and capillary electrophoresis.[1–5] These applications often involve the shearing of tethered polymers. Although such applications are widespread, the nonequilibrium dynamics of sheared polymer chains are little understood. Experimental research has predominantly focused on the measurement of rheological properties or the scattering of light or neutrons in polymer solution.[6] Because there is no direct observation of the microscopic dynamics of polymer under shear, simulation is important to predict the molecular dynamics of polymer in the shear flow.[7] The simulation and numerical calculation mainly focus on the average chain properties.[8–11] The flow of dilute polymer solutions shows some interesting macroscopic effects, including viscosity, enhanced normal stress, and turbulent drag reduction.[12] This non-Newtonian fluid property contributes to the change of polymer conformation by shear.[7,13,14] It has also been found that a change in the polymer configuration is directly related to the shearing force.[7]

The adsorption of polymer chains onto a solid surface has been extensively studied by theoretical,[15,16] numerical,[17–20] and experimental methods.[21,22] Recently, study of the effect of driving force on an end-grafted polymers is of considerable interest.[23–26] The external driving force applied to the polymer can affect the adsorption behaviors as well as the conformational properties of polymer chain.[24–26] There is a critical force as a function of temperature below the critical adsorption temperature for the second-order phase transition (thermal desorption) and the first-order phase transition (mechanical desorption) in the adsorption-desorption phase diagram.[26] The polymer remains adsorbed below the critical force and is desorbed above the critical force. Typical conformations of polymer in the phase diagram for different values of adsorption strength and driving force are exhibiting as isotropic phase, stretched phase and adsorbed phase, respectively.[23] Pulling polymer by one end perpendicular to the surface can usually reduce the adsorption of the polymer, whereas pulling parallel to the surface can promote adsorption of polymer.[27] In the simulation of the effect of lateral force on one end of the polymer, the force flattens polymer perpendicular to the direction of the external force as achieved in the atomic force microscope tensile experiments.[28] In addition, shear flow has different effects on the

* Corresponding authors, E-mail: lihong@wzu.edu.cn (H.L.)
E-mail: xqzhang@wzu.edu.cn (X.Q.Z.)
E-mail: luomengbo@zju.edu.cn (M.B.L)

Received May 18, 2020; Accepted August 3, 2020; Published online October 7, 2020

adsorption of polymer. For free flexible polymers, the number of surface contacts decreases as shear strength is increased until complete desorption occurs,[29] whereas for end-tethered polymers, the stretch of polymer is depressed by the surface attraction, but the adsorption of polymer is enhanced by the shear flow.[30] However, the mechanisms of polymer adsorption under the surface-parallel driving force (or flow) is not clear yet. The above research has inspired us to explore the effect of the external driving force on the adsorption and conformational properties of polymers.

Due to high viscosity, the motion of polymer is mainly in the form of laminar flow.[31] The solid surface produces friction resistance to the flow, resulting in a shear field in the vicinity of the surface. Couette shear flow has uniform shear stress and velocity gradient along the direction perpendicular to the surface.[31] The Oldroyd-B model separates the activation and velocity aspects of shear flow in the constitutive equation,[32] which is helpful in understanding the non-Newtonian fluid behavior of various complex fluids in the shear field. Therefore, it is necessary to understand the deformation of polymer in shear flow at the molecular level. Molecular simulation has become an important tool in the study of polymer shear flow besides experiment and theory.[12,33] The worm like chain (WLC) model is suitable for describing the conformational properties of polymers ranging from flexible to rigid rod with characteristic bending energy.[34] The freely jointed chain (FJC) model is suitable for understanding flexible polymer chains.[35] Polymer fluid assumes that the momentum of moving particles is immediately damped by local thermal fluctuations.[31] Monte Carlo (MC) simulation is used in this work to simulate Couette shear flow by using a uniform driving force and no velocity gradient in the simulation. The simulation is equivalent to adding an electric field parallel to the surface where all the monomers are subject to a constant external force, which is different from the shear flow. Moreover, the adsorbed polymer is relatively thin, thus the shear can be considered as an approximate constant for the adsorbed polymer on the surface.

In this study, we aim to gain a comprehensive understanding of the adsorption and conformation properties of tethered polymers under the uniform driving force parallel to a flat attractive surface. The structure of this paper is organized as follows. In the second section, we introduce the simulation model and calculation method. In the third section, we discuss the results for the adsorption and conformation of polymer under a driving force. Finally, we conclude our main results in the last section.

SIMULATION MODEL AND CALCULATION METHOD

In this work, a single linear chain embedded in a cubic lattice was used for simulating the case of a dilute polymer solution. Its schematic diagram is shown in Fig. 1. The polymer chain consisted of N monomers linked together with the bond from the set (1, 0, 0), (1, 1, 0), (1, 1, 1) by symmetry operations in the simple cubic lattice,[36,37] where the lattice constant d was set as the unit of length, as shown in Fig. 1(a). The system sizes in the x and y directions were larger than the polymer length N. Periodic boundary condition (PBC) was adopted for the system along the x and y directions to mimic a large surface. An attractive surface was placed at layer z=0, and the polymer was placed above the surface from layer z=1, as shown in Figs. 1(b) and 1(c).

A uniform driving force along the positive x direction was applied on all monomers, as shown in Fig. 1(b). Such a driving force leads to a free energy drop $E_1 = -F \cdot \Delta x$ when a monomer moves a distance Δx along the x direction. We also denoted ε as the interaction energy between monomer and

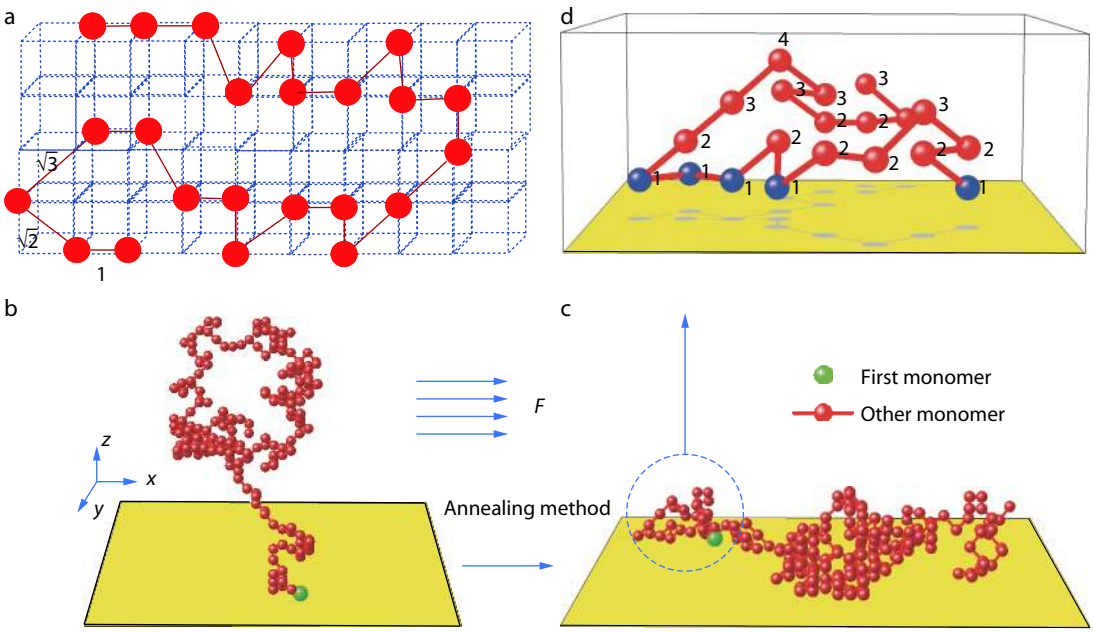

Fig. 1 Schematic of the simulation setup: (a) A single linear chain embedded in a cubic lattice; (b) Polymer above the surface at high temperature above the critical adsorption point (CAP), where the green bead is the first monomer tethered to the surface; (c) Polymer adsorbed on the surface below the CAP; (d) Monomers contact to the surface (the blue beads).

https://doi.org/10.1007/s10118-020-2491-x

surface when the monomer was in contact with the surface, *i.e.*, when the monomer was located on the layer z=1, as shown in Fig. 1(d). The monomer on layer z=1 provided a surface contact. The contact energy of polymer is $E_2 = M\varepsilon$, with M denoting the number of surface contacts. In the simulation, ε/k_B was set as the unit of temperature, with k_B the Boltzmann constant. While interactions between any two of the non-bonded monomers are self-avoiding, bond crossings were allowed, resulting in a high mobility of polymer chains in the simulation.

At the beginning of simulations, an end-tethered polymer chain was generated using the Rosenbluth-Rosenbluth method,[38] with the first monomer located on the position (0, 0, 1) contacted to the surface. The first monomer was restricted to the first layer. In order to investigate the dynamics of polymer on the surface, the first monomer was allowed to move on the first layer, as shown in Fig. 1(b). The polymer chain underwent a series of moves due to the thermal fluctuation and the external driving force. A monomer was picked up randomly and attempted to move to one of its six nearest neighbors, excluding the first monomer confined on the first layer. This trial move was accepted if the following four conditions were simultaneously satisfied: (1) The new site was above the surface (z>0); (2) it fulfilled the self-avoiding condition (any lattice site can be occupied by no more than one monomer); (3) all bond vectors were within bond lengths$\{1,\sqrt{2},\sqrt{3}\}$, (4) the Boltzmann factor was fulfilled according to $\exp(-\Delta E/(k_BT)) > p$, where ΔE is the energy shift due to the move and p is a random number with $0<p<1$. For the move of a monomer, the energy shift ΔE can be expressed as $\Delta E = \Delta E_1 + \Delta E_2$, where $\Delta E_1 = \alpha Fd$, $\Delta E_2 = \beta\varepsilon$. The values of α and β can be taken as 1, 0, and −1 for the increase, invariance, and decrease of the energy, respectively. The parameter α depends on the direction of movement, and β depends on the behavior of adsorption and desorption. Therefore, the probability of accepting the move

$$p = \exp(-\frac{\Delta E}{k_BT}) = \exp(-\frac{\alpha Fd + \beta\varepsilon}{k_BT}) \quad (1)$$

is dependent on F and T in the MC simulation, and the properties of polymer are also dependent on F and T. In one MC step (MCS), all the monomers in polymer chains attempt to move once on average.

We adopted an MC simulated annealing method[19] to investigate polymer properties by decreasing the temperature from T=8 to T=0.05. The temperature step ΔT=0.05 was chosen near the critical adsorption point (CAP), and a slightly greater value of ΔT was adopted away from the CAP. The final configuration at the previous temperature was used as the initial configuration for the current temperature. At each T, we used about $\tau = 2.5N^{2.13}$ MCS to equilibrate the polymer.[37,39] Then, conformations of polymer were recorded at an interval of 0.1τ MCS for the next 100τ MCS. In the simulations, more than 1000 independent runs were implemented, then the results were averaged over 10^6 independent configurations.

RESULTS AND DISCUSSION

For clarity, we summarize our main results by presenting the conformations of polymer chains for different driving force F and temperature T values. Fig. 2 shows the sketches of two-dimensional (2D) projection of conformations. Circle or oval circle represents the projection of polymer on the surface, including its size and orientation. The circle indicates that its projection is uniform in all directions, while the ellipse indicates that its projection orientation is anisotropic. The circular projection depends on the temperature and is almost independent of the driving force F. The size and orientation of the elliptical projection depend on the driving force F and the temperature T. In Fig. 2, the dash curve $F_1(T)$ is the critical force that affects the projection orientation of polymer. When $F<F_1(T)$, the driving force has no effect on the orientation of polymer, otherwise it will deform the polymer. The solid curve $F_2(T)$ is the critical force to make the long axis orientation of the projection consistent with the direction of the driving force F. When $F>F_2(T)$, the polymer will extend along the direction of the driving force F. When $F_1(T)<F<F_2(T)$, the conformation of polymer depends on F and T. The CAP (T_c), which separates the adsorbed polymer and desorbed one, decreases with increasing driving force F. The influence of driving force F on the size and orientation of the desorbed and adsorbed conformations is mainly divided into three main regions: a force dominated (FD) region at strong driving force $F>F_2(T)$, a temperature dominated (TD) region at weak driving force $F<F_1(T)$, and a force-temperature competition-cooperation (FTCC) region at driving force $F_1(T)<F<F_2(T)$. In the TD region, the projection of the polymer was uniform in all orientations, and the area of projection increased with decreasing temperature. In the FD region, the polymer is stretched into an asymmetric profile due to the driving force. The projection of the polymer is elliptical, and the direction of its long axis is the same as that of the external force F. With the decrease of temperature, the degree

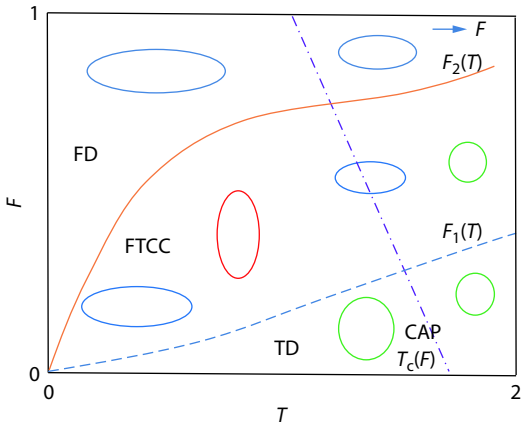

Fig. 2 Sketches of the 2D projection of conformations of polymer on the surface under action of various strengths of driving force (F) at different temperatures (T). Circles or oval circles represent the size and orientation of the projection, where the direction of the force F is horizontal to the right. Three main regions: force dominated (FD) region above the solid curve $F_2(T)$, temperature dominated (TD) region under the dash curve $F_1(T)$, and force-temperature competition-cooperation (FTCC) region between $F_1(T)$ and $F_2(T)$, are illustrated. $T_c(F)$ is the critical adsorption temperature (CAP) of the polymer, where the left is the adsorption state and the right is the desorbed state.

https://doi.org/10.1007/s10118-020-2491-x

of polymer stretching increases. This phenomenon has previously been observed for polymer in solution.[40] However, in the FTCC region, with the decrease of temperature, the orientation of the polymer experienced four different temperature regions as follows. At the high temperature ($T>T_c$), the projection of polymer was also uniform. Near the CAP ($T\rightarrow T_c$), the projection of polymer was slightly stretched along the force direction. At the temperature below CAP ($T<T_c$), the projection of polymer was slightly stretched in the direction normal to the driving force. However, at the temperature close to zero ($T\rightarrow 0$), the projection of polymer was also stretched along the driving force direction. The details of adsorption and conformation properties of polymer under the action of the driving force parallel to the attractive surface are described as follows.

Critical Adsorption of Polymers

We investigated the adsorption behavior of polymer chain onto the surface under the action of the driving force in this work. We calculated the average fraction of surface contacts $<M>/N$, where $<M>$ is the mean number of surface contacts. The fraction $<M>/N$ can be viewed as an order parameter for the degree of adsorption. The CAP of infinitely long polymers can be determined by analyzing the behavior of the $<M>$ of finitely long polymers at different temperatures.[41] The CAP (T_c) of the polymer was expected to be determined by the finite-size scaling theory. Near CAP, the order parameter $<M>/N$ can be expressed as:[42]

$$< M > /N = N^{\phi-1}\left(a_0 + a_1\kappa N^{1/\delta} + O\left(\left(\kappa N^{1/\delta}\right)^2\right)\right) \qquad (2)$$

where ϕ is the crossover exponent, $\kappa = (T - T_c)/T_c$ is the scaled temperature, and $1/\delta$ is the critical exponent that is adopted for $1/\delta = \phi$ in the EKB.[43] The second term $\kappa N^{1/\delta}$ in Eq. (2) changes sign at the temperature T when annealed from $T>T_c$ to $T<T_c$.

Fig. 3(a) shows the dependence of $<M>/N$ on N at different temperatures near the CAP for weak driving force F=0.1. It can be observed from the figure that $<M>/N$-N curves are slightly upward concave at low temperatures and downward convex at high temperatures. Meanwhile, $<M>/N$ shows the best power law behavior at $T=T_c$, which can be expressed as:[43]

$$< M >/N = a_0 N^{\phi-1} \qquad (3)$$

Therefore, T_c and ϕ, which characterize the polymer adsorption transition, can be estimated by searching the best matched power law behavior using Eq. (3). Values of $<M>$ at other temperatures near T_c were obtained by interpolation treatment from the simulation data, and T_c=1.67 and ϕ=0.52 for an infinitely long polymer were found at F=0.1. We obtained nearly the same values of T_c and ϕ at F=0 (not included) by the same method. Our results are roughly the same as that for end-grafted polymer without driving force.[41]

In the TD region, as a result of the weak driving force and the dominant temperature, the CAP (T_c) could be estimated by the finite-size scaling method. However, in the FTCC and FD regions, as a result of the coaction of the external driving force and temperature, T_c could not be determined by the finite-size scaling method as none of the temperature values satisfied the function in Eq. (3), as shown in Fig. 3(b) for F=1.0. At F=1.0, we only find downward convex curves.

In the context of discussing adsorption and conformation of polymer, the finite chain length is also of considerable interest. In the following, the chain length N=200 was taken as an example, and the results of other large N also exhibited similar qualitative behaviors. Additionally, T_c was estimated from the energy fluctuation.

Energy fluctuations, similar to the heat capacity, can provide useful information for the adsorption transition.[44] The transition point can be determined from the position of the maximum value in the contact energy fluctuations represented as $\delta M^2 = <M^2> - <M>^2$ for $E = \varepsilon M$. The peak of the fluctuation δM^2 corresponds to the critical adsorption temperature $T_c(F)$ for the finite chain length.[18,31] The results of δM^2 for N=200 and for different values of driving force F=0, 0.3, 0.5, 0, 8, 1, and 1.2, are depicted in Fig. 4. The estimated values of $T_c(F)$ are presented in the inset of Fig. 4. It can be clearly seen that $T_c(F)$ decreased nearly linearly with increasing external driving force F.

The dependence of the average fraction of surface contact $<M>/N$ on temperature T is shown in Fig. 5 for different driving forces F=0, 0.5, and 1.0, and for chain length N=200. The

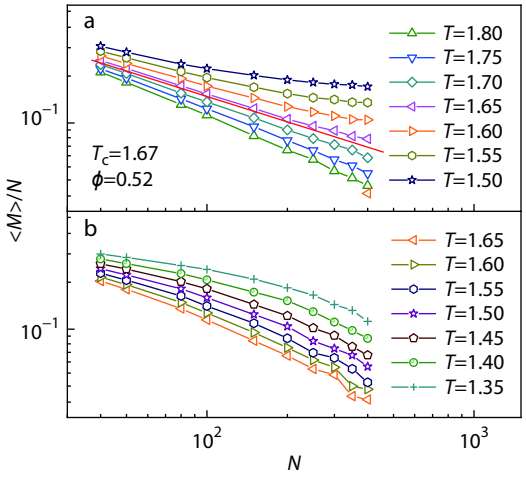

Fig. 3 The log-log plot of $<M>/N$ versus N for various values of driving force (a) F=0.1 and (b) F=1.0 at temperatures from T=1.35 to T=1.80. Chain lengths vary from N=40 to N=400. For T_c=1.67, the mean value of the best slope is depicted for F=0.1 (a).

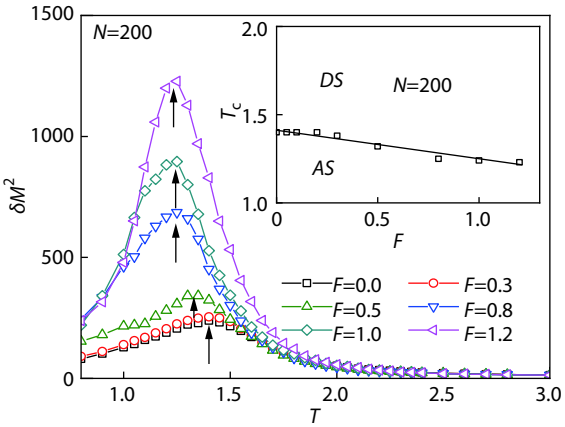

Fig. 4 Contact fluctuations in different temperatures. The inset shows the dependence of the transition point on the driving force for N=200.

https://doi.org/10.1007/s10118-020-2491-x

value of $<M>/N$ ranged from 0 at high temperatures ($T>T_c$) to 1 at the temperature close to zero ($T\to0$). At the intermediate temperatures, $<M>$ increased monotonously with decreasing temperature T. However, there were two intermediate temperature regions. In one region, $<M>$ increased with increasing driving force F at the temperature near the CAP ($T\to T_c$), and in the other region $<M>$ decreased as the F increased at the temperature below the CAP ($T<T_c$). The dependency of the ratio $<M>_F/<M>_{F=0}$ on the driving force F for T=3.0, 1.5, 0.8, and 0.2 is shown in the inset of Fig. 5. At high temperature T=3.0 ($T>T_c$) and close to the zero temperature ($T\to0$) for T=0.2, values of the ratio $<M>_F/<M>_{F=0}$ were roughly equal to 1. At the CAP and below, the ratio $<M>_F/<M>_{F=0}$ was also equal to 1 for the weak driving force. However, the ratio decreased with increasing driving force F for T=1.5 near the CAP ($T\to T_c$), but increased with increasing force F for T=0.8 below the CAP ($T<T_c$). That is, under the driving force, the polymers prefer to be adsorbed on the surface at the temperature below CAP ($T<T_c$), whereas polymers prefer to be desorbed from the surface at the temperature near CAP ($T\to T_c$). Our results indicate that the adsorption properties are not only dependent on temperature T, but also dependent on the driving force F.

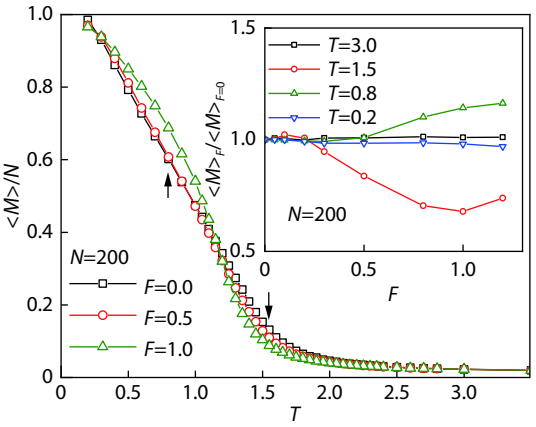

Fig. 5 The average fraction of surface contact as a function of the temperature for the chain length N=200 under action of different values of driving forces F=0, 0.5, and 1. The dependence of ratio $<M>_F/<M>_{F=0}$ on the driving force F for T=3.0, 1.5, 0.8, and 0.2 is presented in the inset.

Conformation Properties of Polymers

It is also interesting to understand the conformation properties of polymer under the external driving force. In this subsection, we studied the mean-square radius of gyration and its three components along x, y, and z directions. The mean-square radius of gyration was calculated as:

$$< R_G^2(N) >= \frac{1}{N}\sum_{i=1}^{N}(\vec{r}_i - \vec{r}_{cm})^2 \quad (4)$$

with

$$\vec{r}_{cm} = \frac{1}{N}\sum_{i=1}^{N}\vec{r}_i \quad (5)$$

The polymers were rearranged from a three-dimensional (3D) structure above T_c to a 2D structure below T_c, which was depicted by the conformation properties changing in the direction perpendicular to the surface. The dependence of the z component of the mean-square gyration radius $\langle R_G^2\rangle_z$ on temperature T is shown in Fig. 6 for polymer N=200 at different forces F=0, 0.3, 0.5, 0.8, and 1.0. The critical transition temperature $T_c(F)$ decreased with increasing driving force F, as shown in the inset of Fig. 6. The value of $T_c(F)$ was estimated as the value of the maximum derivation in the curve $\langle R_G^2\rangle_z$-T, and the results were in good agreement with the critical adsorption temperature calculated from the surface contact number.

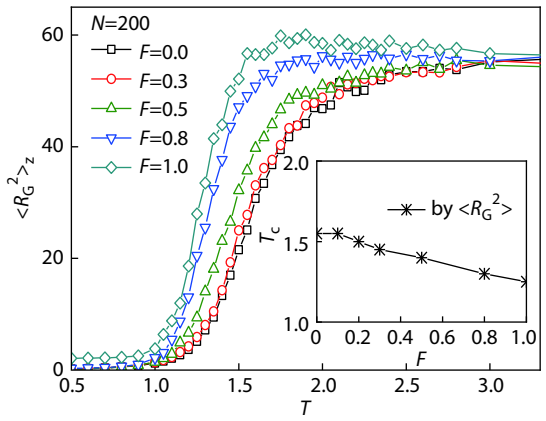

Fig. 6 Temperature dependency of the z component of the mean-square radius of gyration. The inset is the dependency of the transition temperature on the driving force.

To compare the force-parallel-conformation with the force-perpendicular-conformation, the dependency of x, y components of $\langle R_G^2\rangle$, *i.e.*, $\langle R_G^2\rangle_x$ and $\langle R_G^2\rangle_y$ on F is shown in Fig. 7 for N=200. There were two different conformation behaviors of $\langle R_G^2\rangle_x$ and $\langle R_G^2\rangle_y$ with increasing driving force F. One behavior was the change from stretched state in the perpendicular direction $\left(\langle R_G^2\rangle_x < \langle R_G^2\rangle_y\right)$ to stretched state in parallel direction $\left(\langle R_G^2\rangle_x > \langle R_G^2\rangle_y\right)$ for T=0.8 below the CAP ($T<T_c$), as shown in Fig. 7(a). The other was the maintaining of a stretched state in the parallel direction $\left(\langle R_G^2\rangle_x > \langle R_G^2\rangle_y\right)$ for T=1.5 near the CAP ($T\to T_c$), as shown in Fig. 7(b). The conformation of the polymer chain was stretched in different directions at the temperature near the CAP and below under action of the weak driving force F<0.5. This was due to the competition and cooperation between the driving force and temperature for polymer in the FTCC region. However, under strong driving force F>0.5, the polymer chain stayed stretched in the force direction for both temperatures near the CAP and below due to the driving force dominating polymer in the FD region.

When annealing from high to low temperature, the conformations of polymer chains change from a random coil state in the 3D space to stretched adsorption state on the 2D surface. In order to further observe the conformational transition of the polymer chain in the FTCC region, we depicted the temperature T dependency of the mean-square radius of gyration $\langle R_G^2\rangle$ for N=200 and F=0.3, as shown in Fig. 8. The

https://doi.org/10.1007/s10118-020-2491-x

plot shows an interesting trend in the values of $\langle R_G^2 \rangle_x$ and $\langle R_G^2 \rangle_y$ that have experienced four regions: $\langle R_G^2 \rangle_x = \langle R_G^2 \rangle_y$ uniformity at high temperature ($T>T_c$), $\langle R_G^2 \rangle_x > \langle R_G^2 \rangle_y$ stretching in x direction at the temperature near CAP ($T \rightarrow T_c$), $\langle R_G^2 \rangle_x < \langle R_G^2 \rangle_y$ stretching in y direction at the temperature below CAP ($T<T_c$), and $\langle R_G^2 \rangle_x > \langle R_G^2 \rangle_y$ stretching in x direction at the temperature close to zero ($T \rightarrow 0$). The four typical temperatures for chain conformations are illustrated in Fig. 9. At high temperature T=2.0 ($T>T_c$), polymers were in a random coil state in 3D conformation; at the temperature near CAP T=1.5 ($T \rightarrow T_c$), polymers began to enter the adsorption state and were slightly stretched along the x direction; at the temperature below CAP T=0.5 ($T<T_c$), polymers were stretched along the y direction; at T=0.2 close to zero temperature ($T \rightarrow 0$), polymers were further stretched along the x direction. The results illustrate an interesting phenomenon that the polymer extended along the direction normal to the driving force for the temperature below CAP ($T<T_c$) due to the competition and cooperation between temperature and driving force.

To illustrate the details of polymer conformation under the action of different values of driving forces, the ratio $\langle R_G^2 \rangle_y / \langle R_G^2 \rangle_x$ of mean gyration radius components is plotted in Fig. 10 for F=0, 0.3, and 0.8. There was a constant ratio $\langle R_G^2 \rangle_y / \langle R_G^2 \rangle_x$=1 in the TD region where the temperature was a dominant influence factor for F=0. Meanwhile, there were two intermediate temperature regions: $\langle R_G^2 \rangle_y / \langle R_G^2 \rangle_x$<1, at the temperature near CAP ($T \rightarrow T_c$), and $\langle R_G^2 \rangle_y / \langle R_G^2 \rangle_x$>1, at the temperature below CAP ($T<T_c$). This was due to the competition and cooperation between temperature and driving force for F=0.3. However, the ratio $\langle R_G^2 \rangle_y / \langle R_G^2 \rangle_x$ decreased monotonically by decreasing T when the driving force was a dominant influence factor for F=0.8. Our results show that the driving force can stretch the polymers parallel or perpendicu-

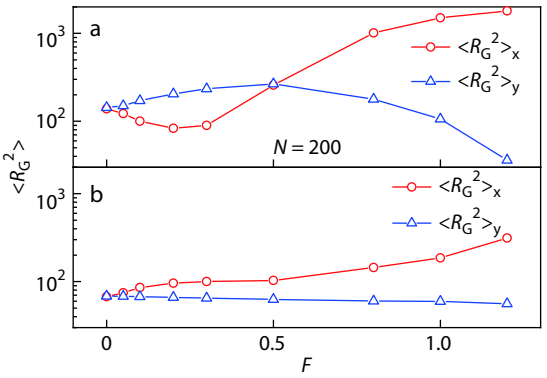

Fig. 7 Dependency of the x- and y-components of the mean-square gyration radius on the driving force: (a) T=0.8 below the CAP; (b) T=1.5 near the CAP.

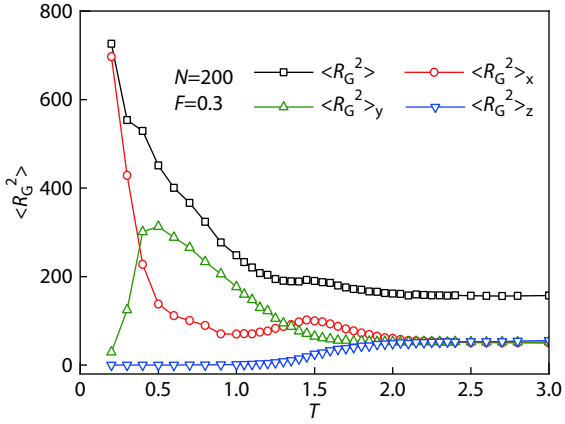

Fig. 8 Dependency of the mean-squared gyration radius $\langle R_G^2 \rangle$ and its three components in x, y, and z direction with the temperature T for F=0.3.

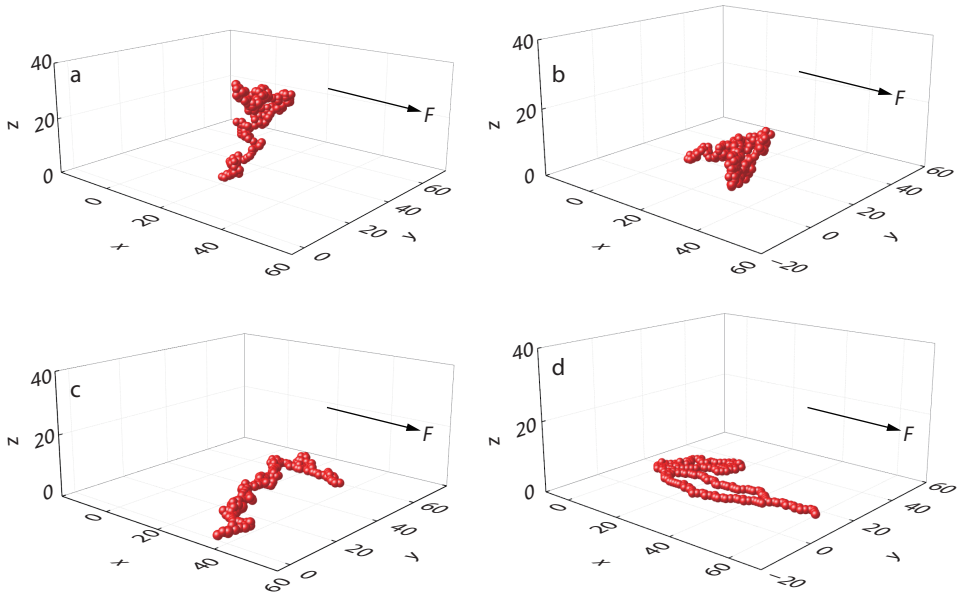

Fig. 9 Typical conformations of polymers at different temperatures: (a) T=2.0; (b) T=1.5; (c) T=0.5; (d) T=0.2 and F=0.3.

https://doi.org/10.1007/s10118-020-2491-x

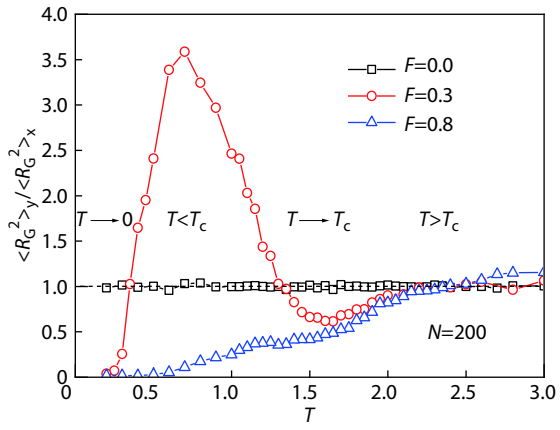

Fig. 10 Plot of the ratio $\langle R_G^2\rangle_y/\langle R_G^2\rangle_x$ versus T for F=0, 0.3, and 0.8.

lar to the direction of the driving force.

However, the stretching effect on polymer chain is dependent on the competition between the driving force and the temperature. The contour plot of the ratio $\langle R_G^2\rangle_y/\langle R_G^2\rangle_x$ versus T and F is presented in Fig. 11. It can be observed that there were three different regions for polymer conformations by factors of driving force and temperature. In the TD region, the ratio $\langle R_G^2\rangle_y/\langle R_G^2\rangle_x$ was close to 1 at small F, and the conformation of the polymer chain was isotropic and could not be stretched by the weak driving force. In the FD region, the ratio $\langle R_G^2\rangle_y/\langle R_G^2\rangle_x$ was less than 1 at strong F, that is to say, the polymer chain was stretched along the direction of the driving force. However, in the intermediate FTCC region, there were different effects on the conformation of polymer at the adsorbed state by the driving force. The polymer chain firstly appeared stretching in the x direction at the temperature near CAP, then appeared stretching in the y direction at the temperature below CAP. This was due to the competition and cooperation between the temperature and driving force.

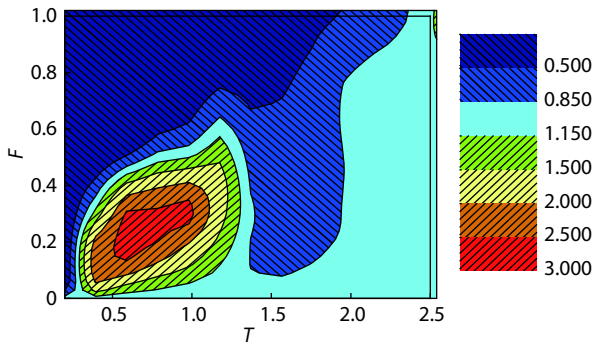

Fig. 11 Contour plots for the ratio, $\langle R_G^2\rangle_y/\langle R_G^2\rangle_x$, of mean-square gyration radius components as a function of temperature T and driving force F.

Orientation of Polymers

The orientation of polymer is generally related to conformation. To further investigate the orientation of polymer influenced by the driving force in the FTCC region, we calculated the eigenvalues of the radius of gyration tensor[45–49]

$$S = \frac{1}{n}\sum_{i=1}^{n} s_i s_i^{\mathrm{T}} = \begin{pmatrix} S_{xx} & S_{xy} & S_{xz} \\ S_{xy} & S_{yy} & S_{yz} \\ S_{xz} & S_{yz} & S_{zz} \end{pmatrix} \quad (6)$$

in 3D space, where s_i = col(x_i, y_i, z_i) was the position of the i^{th} monomer in a frame of reference with its origin at the center of mass. We calculated the orientational behavior of polymer chain by angles of θ_x, θ_y, and θ_z, which were the angles between the eigenvector of the gyration tensor with the largest eigenvalue and the coordinate axis x, y, and z, respectively. The dependence of the angle θ_x, θ_y, and θ_z on T is plotted for F=0.3 and N=200 in Fig. 12. At the high temperature (T>>T_c), the angles θ_x, θ_y, and θ_z were almost equal to the same value $\cos^2\theta = 1/3$, that is, they were almost not influenced by the driving force. At the temperature near CAP ($T\to T_c$), $\cos^2\theta_z$ decreased from 1/3 to 0 as temperature decreased. Meanwhile, $\cos^2\theta_x$ and $\cos^2\theta_y$ increased from 1/3 to 1/2 with the decrease of the temperature, but $\cos^2\theta_x$ and $\cos^2\theta_y$ had different variations due to the competition and cooperation between T and F. At the temperature below CAP (T<<T_c), $\cos^2\theta_x$=$\cos^2\theta_y$=1/2 and $\cos^2\theta_z$=0 for F=0 due to isotropy (not shown). However, the statistical conformation deviated from spherical symmetry and $\cos^2\theta_x$ and $\cos^2\theta_y$ deviated from 1/2 for F=0.3. At the temperature close to zero ($T\to 0$), $\cos^2\theta_x$ was close to 1, indicating that the polymer was stretched in the x direction for F=0.3. As the temperature decreased, the orientation angle of the polymer shown in Fig. 12 was consistent with the components of the mean-square radius of gyration in Fig. 8.

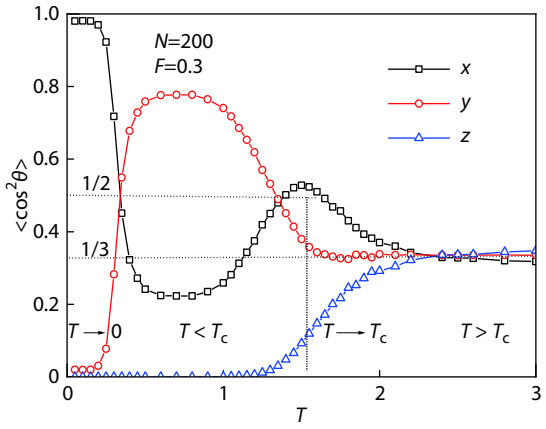

Fig. 12 The angle between the instantaneous largest eigenvector of the gyration tensor and coordinate axis.

In the FTCC region, the polymer chain was adsorbed on the surface and was also driven by the external force F parallel to the surface. The polymer was not conducive to the movement of desorption from the surface, or the movement in the opposite direction of the driving force. In this region, the polymer chain extended along the direction normal to the driving force due to the competition and cooperation between the driving force and the surface attraction, so as to achieve synchronous movement along the direction of the driving force. This behavior qualitatively occurred when polymers were deformed by the driving force and the surface adsorption (See Fig. 8). The extension of polymer along the direction normal to the driving force could be attributed to

https://doi.org/10.1007/s10118-020-2491-x

the Brownian motion, which attempts to randomize the polymer chain and bring it back to an undeformed state.

CONCLUSIONS

In our work, the adsorption and conformation of polymers under the action of driving force parallel to the surface were studied by employing Monte Carlo simulations. The critical adsorption temperature T_c and the crossover exponent ϕ were estimated from the scaling relation between the number of surface contacts and the chain length for the weak driving force. With the increase of driving force F, we found that T_c for an infinitely long polymer cannot be determined by finite-size scaling relations. However, finite chain length is also of considerable interest when discussing the adsorption and conformation of polymer. $T_c(F)$ was roughly determined by the variance of surface contact for finitely long polymers, and we found that T_c decreased with the increase of the driving force F. The conformation of polymer under driving force had three different variation tendencies with the annealing temperature. The conformation of polymer was isotropic parallel to the surface in the TD region and was stretched in the driving force direction in the FD region. However, in the FTCC region, the conformation of polymer experienced four different cases, isotropic at high temperature above CAP, stretched in the driving force direction at the temperature near CAP, stretched in the perpendicular driving force direction at the temperature below CAP, and further stretched along the driving force direction at the temperature close to zero. These results are consistent with the orientation angles between the largest eigenvector and coordinate axis. Moreover, the polymer chains were stretched perpendicular to the driving force direction so that monomers could move synchronously along the driving force direction on the surface due to the normal stress bringing the polymer back to an undeformed state.

ACKNOWLEDGMENTS

This work was financially supported by the Research Fund of Zhejiang Provincial Education Department (No. Y201738867) and the National Natural Science Foundation of China (Nos. 11775161, 11875205, and 11974305).

REFERENCES

1 Smith, P.; Ziolek, R. M.; Gazzarrini, E.; Owen, D. M.; Lorenz, C. D. On the interaction of hyaluronic acid with synovial fluid lipid membranes. *Phys. Chem. Chem. Phys.* **2019**, *21*, 9845–9857.
2 Yan, W.; Ramakrishna, S. N.; Romio, M.; Benetti, E. M. Bioinert and lubricious surfaces by macromolecular design. *Langmuir* **2019**, *35*, 13521–13535.
3 Morales, M. A.; Paiva, W. A.; Marvin, L.; Balog, E. R. M.; Halpern, J. M. Electrochemical characterization of the stimuli-response of surface-immobilized elastin-like polymers. *Soft Matter* **2019**, *15*, 9640–9646.
4 Xia, Y. Q.; Tian, W. D.; Chen, K.; Ma, Y. Q. Globule-stretch transition of a self-attracting chain in the repulsive active particle bath. *Phys. Chem. Chem. Phys.* **2019**, *21*, 4487–4493.
5 Rao, A. N.; Grainger, D. W. Biophysical properties of nucleic acids at surfaces relevant to microarray performance. *Biomater. Sci.* **2014**, *2*, 436–471.
6 Smith, D. E.; Babcock, H. P.; Chu, S. Single-polymer dynamics in steady shear flow. *Science* **1999**, *283*, 1724–1727.
7 Chen, W.; Li, Y.; Zhao, H.; Liu, L.; Chen, J.; An, L. Conformations and dynamics of single flexible ring polymers in simple shear flow. *Polymer* **2015**, *64*, 93–99.
8 He, G. L.; Messina, R.; Löwen, H.; Kiriy, A.; Bocharova, V.; Stamm, M. Shear-induced stretching of adsorbed polymer chains. *Soft Matter* **2009**, *5*, 3014–3017.
9 He, G. L.; Messina, R.; Lowen, H. Statistics of polymer adsorption under shear flow. *J. Chem. Phys.* **2010**, *132*, 124903.
10 Li, H.; Qian, C. J.; Luo, M. B. Critical adsorption of copolymer tethered on selective surfaces. *J. Chem. Phys.* **2016**, *144*, 164901.
11 Li, H.; Qian, C. J.; Sun, L. Z.; Luo, M. B. Conformational properties of a polymer tethered to an interacting flat surface. *Polym. J.* **2010**, *42*, 383–385.
12 Baig, C.; Mavrantzas, V. G.; Kröger, M. Flow effects on melt structure and entanglement network of linear polymers: results from a nonequilibrium molecular dynamics simulation study of a polyethylene melt in steady shear. *Macromolecules* **2010**, *43*, 6886–6902.
13 O'Connor, T. C.; Alvarez, N. J.; Robbins, M. O. Relating chain conformations to extensional stress in entangled polymer melts. *Phys. Rev. Lett.* **2018**, *121*, 047801.
14 Lu, Y.; An, L.; Wang, S. Q.; Wang, Z. G. Evolution of chain conformation and entanglements during startup shear. *ACS Macro Lett.* **2013**, *2*, 561–565.
15 De Gennes, P. G. Scaling theory of polymer adsorption. *J. Phys.* **1976**, *37*, 1445–1452.
16 Migliorini, E.; Weidenhaupt, M.; Picart, C. Practical guide to characterize biomolecule adsorption on solid surfaces. *Biointerphases* **2018**, *13*, 06D303.
17 Li, H.; Qian, C. J.; Huang, J. H.; Luo, M. B. Critical adsorption of an end-grafted diblock copolymer on a flat surface. *Polym. J.* **2015**, *47*, 53–58.
18 Yang, X.; Yang, Q. H.; Fu, Y.; Wu, F.; Huang, J. H.; Luo, M. B. Study on the adsorption process of a semi-flexible polymer onto homogeneous attractive surfaces. *Polymer* **2019**, *172*, 83–90.
19 Li, H.; Gong, B.; Qian, C. J.; Luo, M. B. Critical adsorption of a flexible polymer on a stripe-patterned surface. *Soft Matter* **2015**, *11*, 3222–3231.
20 Sun, L. W.; Li, H.; Zhang, X. Q.; Gao, H. B.; Luo, M. B. Identifying conformation states of polymer through unsupervised machine learning. *Chinese J. Polym. Sci.* **2020**, *38*, 1403–1408.
21 Maroni, P.; Montes Ruiz-Cabello, F. J.; Cardoso, C.; Tiraferri, A. Adsorbed mass of polymers on self-assembled monolayers: effect of surface chemistry and polymer charge. *Langmuir* **2015**, *31*, 6045–6054.
22 Luo, R.; Jiang, H.; Du, B.; Zhou, S.; Zhu, Y. Preparation and application of solid polymer electrolyte based on deep eutectic solvent. *AIP Adv.* **2019**, *9*, 035341.
23 Skvortsov, A. M.; Gorbunov, A. A.; Klushin, L. I. Adsorption-stretching analogy for a polymer chain on a plane. Symmetry property of the phase diagram. *J. Chem. Phys.* **1994**, *100*, 2325.
24 van Rensburg, E. J. J.; Whittington, S. G. Adsorbed self-avoiding walks subject to a force. *J. Phys. A: Mathemat. Theor.* **2013**, *46*, 435003.
25 Iliev, G. K.; Whittington, S. G. Adsorbed polymers on an inhomogeneous surface: pulling at an angle. *J. Phys. A: Mathemat. Theor.* **2012**, *45*, 185003.
26 Skvortsov, A. M.; Klushin, L. I.; Fleer, G. J.; Leermakers, F. A. Analytical theory of finite-size effects in mechanical desorption of a polymer chain. *J. Chem. Phys.* **2010**, *132*, 064110.
27 Orlandini, E.; Whittington, S. G. Adsorbing polymers subject to an elongational force: the effect of pulling direction. *J. Phys. A: Mathemat. Theor.* **2010**, *43*, 485005.
28 Serr, A.; Netz, R. R. Enhancing polymer adsorption by lateral

pulling. *Europhys. Lett.* **2007**, *78*, 68006.
29 Dutta, S.; Dorfman, K. D.; Kumar, S. Adsorption of single polymer molecules in shear flow near a planar wall. *J. Chem. Phys.* **2013**, *138*, 034905.
30 Ibanez-Garcia, G. O.; Goldstein, P.; Hanna, S. Brownian dynamics simulations of confined tethered polymers in shear flow: the effect of attractive surfaces. *Eur. Phys. J. E* **2013**, *36*, 56.
31 Li, J.; Nie, Y. J.; Ma, Y.; Hu, W. B. Stress-induced polymer deformation in shear flows. *Chinese J. Polym. Sci.* **2013**, *31*, 1590–1598.
32 Li, G.; Ardekani, A. M. Collective motion of microorganisms in a viscoelastic fluid. *Phys. Rev. Lett.* **2016**, *117*, 118001.
33 Kong, X.; Han, Y.; Chen, W.; Cui, F.; Li, Y. Understanding conformational and dynamical evolution of semiflexible polymers in shear flow. *Soft Matter* **2019**, *15*, 6353–6361.
34 Jiang, Y.; Chen, J. Z. Y. The applications of the wormlike chain model on polymer physics. *Acta Phys. Sin.* **2016**, *65*, 17820.
35 Li, Y.; Huang, Q.; Shi, T.; An, L. Effects of chain flexibility on polymer conformation in dilute solution studied by lattice Monte Carlo simulation. *J. Phys. Chem. B* **2006**, *110*, 3502–23506.
36 Shaffer, J. S. Effects of chain topology on polymer dynamics: bulk melts. *J. Chem. Phys.* **1994**, *101*, 4205–4213.
37 Li, H.; Qian, C. J.; Wang, C.; Luo, M. B. Critical adsorption of a flexible polymer confined between two parallel interacting surfaces. *Phys. Rev. E* **2013**, *87*, 012602.
38 Rosenbluth, M. N.; Rosenbluth, A. W. Monte Carlo calculation of the average extension of molecular chains. *J. Chem. Phys.* **1955**, *23*, 356–359.
39 Li, H.; Gong, B.; Qian, C. J.; Li, C. Y.; Huang, J. H.; Luo, M. B. Simulation of conformational properties of end-grafted diblock copolymers. *RSC Adv.* **2014**, *4*, 27393–27398.
40 Li, J.; Ma, Y.; Hu, W. Dynamic Monte Carlo simulation of non-equilibrium Brownian diffusion of single-chain macromolecules. *Molecul. Simul.* **2015**, *42*, 321–327.
41 Li, H.; Qian, C. J.; Luo, M. B. Simulation of a flexible polymer tethered to a flat adsorbing surface. *J. Appl. Polym. Sci.* **2012**, *124*, 282–287.
42 Luo, M. B. The critical adsorption point of self-avoiding walks: a finite-size scaling approach. *J. Chem. Phys.* **2008**, *128*, 044912.
43 Eisenriegler, E.; Kremer, K.; Binder, K. Adsorption of polymer chains at surfaces: scaling and Monte Carlo analyses. *J. Chem. Phys.* **1982**, *77*, 6296–6320.
44 Sumithra, K. The influence of adsorbate-surface interaction energy on adsorption and recognition of diblock copolymers on patterned surfaces. *J. Chem. Phys.* **2009**, *130*, 194903.
45 Zhang, X.; Fan, M.; Wang, D.; Zhou P.; Tao, D. Top-*k* feature selection framework using robust 0-1 integer programming. *IEEE Trans. Neural Netw. Learn. Syst.* **2020**, DOI: 10.1109/TNNLS.2020.3009209.
46 Zhang, X.; Wang, T; Wang, J; Tang, G.; Zhao, L. Pyramid channel-based feature attention network for image dehazing. *Comput. Vis. Image Und.* **2020**, *197-198*, 103003.
47 Zhang, X; Jiang, R.; Wang, T.; Huang, P.; Zhao, L. Attention-based interpolation network for video deblurring. *Neurocomputing* **2020**, DOI: 10.1016/j.neucom.2020.04.147.
48 Zhang, X.; Wang, D.; Zhou, Z.; Ma, Y. Robust low-rank tensor recovery with rectification and alignment. *IEEE Trans. Pattern Anal. Mach. Intell.* **2020**, DOI: 10.1109/TPAMI.2019.2929043.
49 Zhang, X.; Hu, W.; Xie, N.; Bao, H.; Maybank, S. A robust tracking system for low frame rate video. *Int. J. Comput. Vis.* **2015**, *115*, 279–304.

https://doi.org/10.1007/s10118-020-2491-x